Structural Domains of DNA Mesojunctions†

Hui Wang and Nadrian C. Seeman*

Department of Chemistry, New York University, New York, New York 10003

Received September 13, 1994; Revised Manuscript Received November 14, 1994®

ABSTRACT: Holliday junctions are central intermediates in the process of genetic recombination. These DNA molecules contain four double helices that flank a central branch point, so that each of the four strands that constitute the junction is associated with two different helices. Previously, we have shown that such branched junctions are a special subset of the class of DNA molecules containing multiple strands, in which each strand is associated with two double helices [Du, S. M., Zhang, S., & Seeman, N. C. (1992) *Biochemistry 31*, 10955−10963]. Conventional branched molecules, such as the Holliday junction, contain helices whose axes can all be drawn to radiate from a central point. The other molecules of the class contain helices whose axes are circumferential about the central point. If all of the helices are circumferential, the molecule is called an antijunction; if the molecule contains a mixture of radial and circumferential helices, it is called a mesojunction. The properties of the molecule are a function of the even or odd nature of the number of helical half-turns in the circumferential helices. Previously, a four-strand antijunction and three-strand and four-strand mesojunctions containing three half-turns (16 nucleotide pairs) per helix were constructed and characterized. Here, we have attempted to construct the analogous molecules containing two half-turns (10 nucleotide pairs) in each helix. The three-strand mesojunction and the four-strand antijunction are not stable under conditions suitable for analysis. We have characterized the two four-strand mesojunctions that are stable by Ferguson analysis, thermal denaturation, and Fe(II)EDTA^{2-} autofootprinting. In addition, we have characterized a four-strand mesojunction containing 14 nucleotide pairs in its circumferential helices and have shown that its favored conformer is different from that of a closely related molecule containing 16 nucleotide pairs in its circumferential helices.

Nucleic acid structure is a central feature in the molecular basis of biological systems. Ever since the discovery of the DNA double helix (Watson & Crick, 1953), a large variety of secondary structures have been shown to occupy key roles in molecular biology: Triple helical pairing is seen in tRNA (Kim *et al.*, 1974), tetra-G structures appear to be involved in telomeres (Kang *et al.*, 1992; Smith & Feigon, 1992), and pseudoknots are found in mRNA structures (e.g., Tang & Draper, 1989). One particular class of nucleic acid structures contains those molecules whose strands each participate in two different helices. The most prominent member of this class is the Holliday (1964) junction, a four-strand structure known to be involved as an intermediate in site-specific genetic recombination (Hoess *et al.*, 1987; Kitts & Nash, 1987; Nunes-Duby *et al.*, 1987).

The four strands of the Holliday junction are each associated with two double-helical arms. This structure is labeled 4_4 in Figure 1a, which shows it drawn in an unusual representation, with only a single half-turn of duplex DNA per arm. Each helix in this diagram is drawn flanking the corner of a square. The axis of each double helix points radially, along a diagonal of the square, toward its center; the central dyad axis of the half-turn points in a circumferential direction, perpendicular to the radial helix axis. Of the four ends of the two strands that make up each helix, a 5′ end and a 3′ end near the center of the square make connections to adjacent helices, and those farther away contain a free 3′ end and a free 5′ end. The Holliday junction and its analog, the immobile junction (Seeman, 1982), have been characterized extensively in recent years [see reviews by Lilley and Clegg (1993) and Seeman and Kallenbach (1994)]. Branched junctions containing three (Ma *et al.*, 1986), five, and six (Wang *et al.*, 1991) double-helical arms have also been constructed and characterized. The three-arm branched junction is shown with a single half-turn of DNA duplex per arm as the object labeled 3_3 in Figure 1a; its helix axes are coincident with the altitudes of the equilateral triangle it surrounds.

Recently, we have shown that the Holliday junction and other branched junctions comprise a special subset of those multistranded nucleic acid complexes in which each strand participates in two adjacent double helices (Du *et al.*, 1992). The other members of this class are the antijunctions and the mesojunctions. The structure labeled 4_0 in Figure 1a is an antijunction. At first glance, it appears very similar to the junction: Each corner of the square contains a half-turn of DNA, and the half-turns are connected by the strands that make up the complex. However, there has been a reorientation of the helix axes, so that they point in a circumferential direction about the center of the square; it is now the central dyad axes that point radially along the diagonals of the square, toward its center. The four ends of the helical strands are oriented differently, as well: The connections to adjacent helices are both 5′ or 3′ ends, and the free ends are both 3′ ends or 5′ ends, respectively.

If one reorients one of the helices of a junction or an antijunction, 5′−5′ or 3′−3′ linkages will result; these can be accommodated in conventional DNA only by the inclusion

† This research was supported by Grant GM-29554 from the NIH to N.C.S. and by a Margaret and Herman Sokol Fellowship to H.W.

* To whom correspondence should be addressed.

® Abstract published in *Advance ACS Abstracts,* January 1, 1995.

0006-2960/95/0434-920$09.00/0

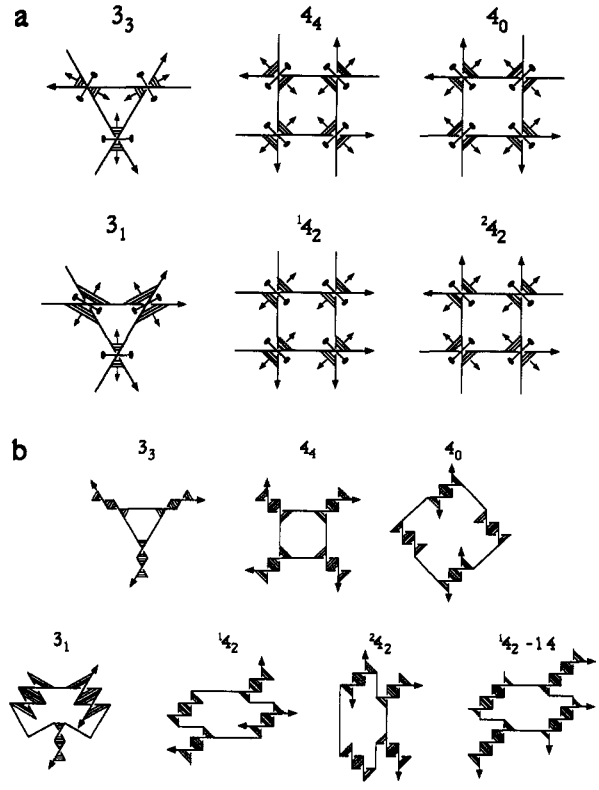

FIGURE 1: Schematic drawings of three-strand and four-strand junctions, antijunctions, and mesojunctions. (a) The helical arrangements that can flank a triangle or a square. Each polygon is formed from strands of DNA that extend beyond the vertices in each direction. The arrowheads indicate the 3′ ends of the strands. The vertices correspond to the nodes formed by approximately a half-turn of double-helical DNA. Base pairs are represented by lines between antiparallel strands. Thin lines ending in arrowheads perpendicular to the base pairs represent the axis of each helical half-turn. The lines perpendicular to the helix axes ending in ovals that pass through the vertices of the polygons represent the central dyad axes of the helical half-turns. The complexes 3_3 and 4_4 correspond to conventional branched junctions. Their helix axes are all pointing toward the center of the triangle or square along the bisectors of the angles of the polygons ("radial"). The complex 4_0 is a four-strand antijunction, in which each helix axis ideally is perpendicular to the angular bisectors ("circumferential"). In this case, the central dyad axes of the helical half-turns are coincident with the diagonals of the square. The complexes are named by a large number which indicates the number of strands (equal to the number of double-helical segments), a subscript which indicates how many of them are pointed along the angular bisectors, and a presuperscript (if necessary) enumerating different members of a class otherwise undifferentiated by the first two numbers. The complexes on the bottom row are mesojunctions, which contain a mix of the two orientations of helix axes. The complex 3_1 contains one radial helix axis and two circumferential axes. The complexes $^1\!4_2$ and $^2\!4_2$, each contain a pair of radial helix axes and a pair of circumferential axes, but the arrangement is different between them: $^1\!4_2$ contains alternating radial and circumferential axes, whereas $^2\!4_2$ contains two radial axes on the right of the square and two circumferential axes on the left. (b) The complexes studied here. Each molecule corresponds to the one with the same label in panel a. However, here we have indicated a full turn of DNA in each double-helical segment, rather than 0.5 turns of DNA, as shown in panel a, except for the seventh member of this panel, labeled $^1\!4_2$-14, which contains 1.5 helical turns of DNA (16 nucleotide pairs in its radial helices and 14 nucleotide pairs in its circumferential helices). The apparent unpaired regions between double helices are artifacts of the representation used and are not designed into the molecules. The structures have been symmetrized somewhat, but no structural implications should be drawn.

of long loops (introducing potentially complex topology) in the structure. However, it is possible to avoid long loops by reorienting the helices in pairs. Thus, it is possible to generate further structures, termed mesojunctions, that mix radial helices and circumferential helices (Du *et al.*, 1992). Figure 1a illustrates the two four-strand mesojunctions, $^1\!4_2$ and $^2\!4_2$, as well as the three-strand mesojunction, 3_1. The large number in this notation represents the number of strands, the subscript indicates the number of radial arms, and the presuperscript is a serial number for those molecules not distinguished by the subscript.

The packing and stacking of circumferential double helices is expected to be sensitive to the twist of the helical components. Hence, the structures of antijunctions and mesojunctions are likely to differ, as a function of the number of helical half-turns of DNA in their circumferential domains (Du *et al.*, 1992): The properties of molecules containing even numbers of half-turns are expected to differ from those containing odd numbers. On the other hand, there is no apparent reason to suspect that changing the lengths of radial arms will effect any structural properties other than the ultimate stability of the molecule. Previously, we have constructed and characterized a three-strand mesojunction, a four-strand antijunction, and two four-strand mesojunctions containing three helical half-turns (16 nucleotides) in their helical domains (Du *et al.*, 1992). These molecules indeed displayed sensitivity to circumferential domain length. For example, the $^2\!4_2$ mesojunction was found not to form a discrete structure, and the $^1\!4_2$ mesojunction had an unusual stacking pattern that could be ascribed to maximizing stacking while minimizing torsional stress.

Here, we have explored the consequences of changing the helices from those containing an odd number of half-turns to those containing an even number of half-turns. We have built the same set of molecules, but now containing two helical half-turns of DNA (10 nucleotides) in each of their helical domains. Schematic diagrams of these molecules are illustrated in Figure 1b. The four-strand antijunction, 4_0, and the three-strand mesojunction, 3_1, do not form stable complexes, but we have been able to construct the four-strand mesojunctions in this group. We have characterized these molecules by nondenaturing gel electrophoresis, Ferguson (1964) analysis, and thermal denaturation; preliminary structural analysis by means of hydroxyl radical autofootprinting analysis (Tullius & Dombroski, 1985, 1986; Churchill *et al.*, 1988) has also been performed. In addition, our previous study (Du *et al.*, 1992) led us to suggest that a three-half-turn $^1\!4_2$ mesojunction containing 14 nucleotides in its circumferential helices (indicated as $^1\!4_2$-14 in Figure 1b) would favor a different stacking isomer from one containing 16 nucleotides in its circumferential helices. We have tested that prediction here and have found it to be correct.

MATERIALS AND METHODS

Sequence Design. The same domain sequences are used for each of the three mesojunctions containing 10 nucleotide pairs per double helical arm. The strands required for the junction and mesojunctions of the set may have their 5′ and 3′ halves reversed. One can represent the sequence of the four strands of the branched junction (4_4) by $1_{5'}1_{3'}$, $2_{5'}2_{3'}$, $3_{5'}3_{3'}$, and $4_{5'}4_{3'}$, where each symbol represents the sequence of a portion of the strand 5′ or 3′ to the branch point. Strands whose sequence is represented by $1_{5'}1_{3'}$, $2_{5'}2_{3'}$, $3_{3'}3_{5'}$, and $4_{3'}4_{5'}$ will produce a $^1\!4_2$ mesojunction. Likewise, $1_{5'}1_{3'}$, $2_{5'}2_{3'}$, $3_{5'}3_{3'}$, and $4_{3'}4_{5'}$ generate a $^2\!4_2$ mesojunction, and $1_{5'}1_{3'}$, $2_{3'}2_{5'}$, $3_{5'}3_{3'}$,

and $4_{3'}4_{5'}$ correspond to an antijunction (4_0). The four nucleotide pairs nearest the branched junction, 4_4, are from the sequence of the well-characterized branched junction J1 (Seeman & Kallenbach, 1983). In a similar fashion, if the sequence of the three-arm branched junction (3_3) is represented by $1_{5'}1_{3'}$, $2_{5'}2_{3'}$, $3_{5'}3_{3'}$, strands with the sequence $1_{5'}1_{3'}$, $2_{5'}2_{3'}$, $3_{3'}3_{5'}$ generate a three-strand mesojunction (3_1). The sequences of the three-strand junction and mesojunction are also derived from our earlier study (Du *et al.*, 1992). The $^14_2$ mesojunction containing 14 nucleotide pairs in its central domains contains the same sequence as the previously characterized $^14_2$ mesojunction containing 16 nucleotide pairs in all domains (Du *et al.*, 1992), except that two nucleotide pairs have been deleted from the middle of each of the central domains.

Synthesis and Purification of DNA. All DNA molecules in this study have been synthesized on an Applied Biosystems 380B automatic DNA synthesizer, removed from the support, and deprotected, using routine phosphoramidite procedures (Caruthers, 1985). DNA strands have been purified by either polyacrylamide gel electrophoresis or by HPLC, using a Du Pont Zorbax Bio Series oligonucleotide column, by means of a gradient of NaCl in a solvent system containing 20% acetonitrile and 80% 0.016 M sodium phosphate, as described previously (Wang *et al.*, 1991).

Formation of Hydrogen-Bonded Complexes. Complexes are formed by mixing a stoichiometric quantity of each strand, as estimated by OD_{260}. This mixture is then heated to 90 °C for 10 min and slowly cooled to the desired temperature. Stoichiometry is estimated by native gel electrophoresis of adjacent dimers that are expected to pair together, such as strands 1 and 2 of the branched junction complex. A single band on a native gel is taken to indicate a homogeneous stoichiometric complex.

Thermal Transition Profiles. Response to increased temperature is measured on a Gilford Response II UV−vis spectrophotometer at 268 nm. Complexes are formed at a concentration of 500 nM for each strand, in a solution containing 40 mM sodium cacodylate, pH 7.0, and 10 mM $MgCl_2$. Temperature is incremented at the rate of 0.1 °C/min.

Hydroxyl Radical Analysis. Individual strands of the complexes are radioactively labeled and are additionally gel purified from a 15% denaturing polyacrylamide gel. Each of the labeled strands is annealed to a 10-fold excess of the unlabeled complementary strands, or it is annealed to a 10-fold excess of a mixture of the other strands forming the complex, or it is left untreated as a control, or it is treated with sequencing reagents (Maxam & Gilbert, 1977) for a sizing ladder. The labeled strand is at a concentration of 10−20 nM, and the unlabeled strands are at a concentration of 100 nM; they are dissolved in 6 μL of a solution containing 40 mM Tris-HCl (pH 7.5), 2 mM EDTA, 20 mM acetic acid, and 10 mM magnesium acetate (TAEMg). The 100 nM concentrations are necessary to ensure that the species under investigation is indeed the sole species present in solution (see below). The samples are annealed by heating to 90 °C for 10 min and then cooled slowly to 4 °C. One microliter of each of Fe(II)EDTA^{2-}, L-ascorbic acid, and H_2O_2 are added to the mixture on ice. Hydroxyl radical cleavage of the double-strand and junction samples for all strands takes place for 2 min (Tullius & Dombroski, 1985), with modifications noted by Churchill *et al.* (1988). The reaction is stopped by addition of 1 μL of thiourea. The sample is ethanol precipitated and then dried, dissolved in a formamide/dye mixture and loaded directly onto a 15% polyacrylamide/8.3 M urea sequencing gel. Autoradiograms are scanned with a Hoefer GS300 densitometer in transmission mode.

Polyacrylamide Gel Electrophoresis. Denaturing Gels. These gels contain 8.3 M urea and are run at 65 °C. Gels contain 15% acrylamide (19:1 acrylamide/bisacrylamide). The running buffer consists of 89 mM Tris-HCl, pH 8.0, 89 mM boric acid, and 2 mM EDTA (TBE). The sample buffer consists of 10 mM NaOH and 1 mM EDTA, containing 90% formamide and 0.1% xylene cyanol FF tracking dye. Gels are run on an IBI Model STS 45 electrophoresis unit at 60 W (45 V/cm), constant power, dried onto Whatman 3MM paper, and exposed to X-ray film with an intensifying screen for up to 15 h.

Nondenaturing Gels. Gels contain 12−15% acrylamide (19:1 acrylamide/bisacrylamide). DNA is suspended in 10 μL of a solution containing 40 mM Tris-HCl, pH 8.0, 20 mM acetic acid, 2 mM EDTA, and 12.5 mM magnesium acetate (TAEMg); the quantities loaded vary as noted below. The solution is boiled and allowed to cool slowly to 4, 25, 37, or 45 °C. Samples are then brought to a final volume of 11 μL with a solution containing TAEMg, 50% glycerol, and 0.02% each of bromophenol blue and xylene cyanol FF tracking dyes. Gels are run on a Hoefer SE-600 gel electrophoresis unit at 8 V/cm at 4, 25, 37, or 45 °C and exposed to X-ray film for up to 15 h or stained with Stainsall dye. Absolute mobilities (cm/h) of native gels run at 4 °C are measured for Ferguson analysis; logarithms are measured to base 10.

RESULTS

Formation of the Complexes. It is necessary to determine whether the structures illustrated in Figure 1 can actually form as discrete complexes. In our previous characterization of mesojunctions and antijunctions (Du *et al.*, 1992), we found that other structures competed with the target structures at high strand concentrations, under conditions that are favorable for the formation of conventional branched junctions (Kallenbach *et al.*, 1983; Wang *et al.*, 1991). We find the same to be true here. Figure 2a illustrates a nondenaturing gel containing stoichiometric mixtures of the appropriate strands at a concentration of 7.5 μM for each of the six possible complexes shown in Figure 1b. Shown from left to right are a marker dimer of two adjacent strands, the 3_1 mesojunction, the 3_3 and 4_4 branched junctions, the $^14_2$ and $^24_2$ mesojunctions, and the 4_0 antijunction. The conventional branched junctions appear as single bands (there is a hint of dimer for 3_3); however, all of the mesojunctions display multimers, although this problem is least severe for $^14_2$. The multimers of the four-stranded complexes appear to have the composition $(1:2:3:4)_n$, and those for the three-strand mesojunction appear to have the composition $(1:2:3)_n$, as estimated from plots of log(putative MW) vs mobility (data not shown). The antijunction appears as a smear; we have previously suggested (Du *et al.*, 1992) that such a smear represents unclosed complexes of indefinite composition (1:2:3:4:1:2:3...), in contrast to discrete closed complexes of definite composition. Thus, the strong extra band in the lane containing the $^24_2$ mesojunction is likely to be a discrete complex with the composition, $(1:2:3:4)_2$. This is not the target molecule, but it appears to have a well-defined composition, unlike the smear seen for the antijunction.

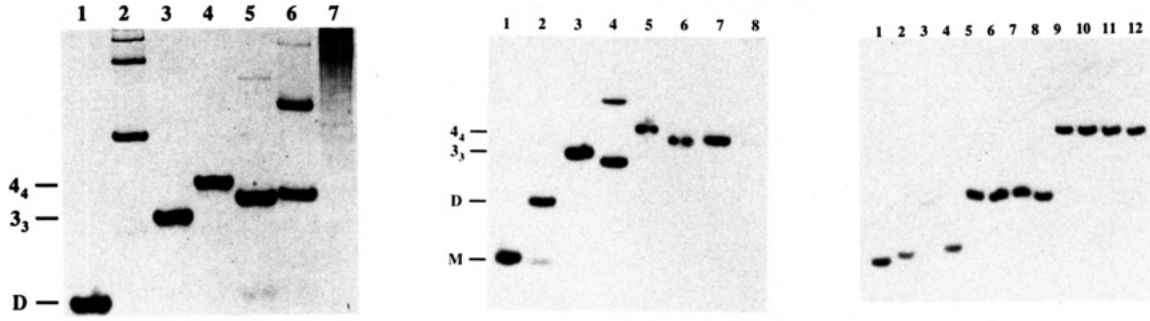

FIGURE 2: Native gels of three-strand and four-strand junctions, antijunctions, and mesojunctions. (a, left) Equimolar mixtures of strands at 7.5 μM strand concentrations, which are electrophoresed at 4 °C. This 15% nondenaturing polyacrylamide gel is stained with Stains-all dye. Lane 1 contains an equimolar mixture of adjacent strands 2 and 3 of the conventional four-arm junction, 4_4, as a marker. Lane 2 contains the components of the 3_1 mesojunction. Lane 3 contains the components of the conventional three-arm junction, 3_3. Note the presence of at least four bands in lane 2, none of which migrate as rapidly the three-arm junction in lane 3. Lane 4 contains the components of the conventional four-arm branched junction, 4_4. Lane 5 contains the components of the $^14_2$ mesojunction. A faint band indicating a multimer is evident above the main band. Lane 6 contains the components of the $^24_2$ mesojunction. Note that two larger species are evident in addition to the target complex. Lane 7 contains the component strands of the 4_0 antijunction. Virtually all of the material migrates in a smear of low mobility. (b, middle) Equimolar mixtures of strands at 100 nM strand concentrations, which are electrophoresed at 4 °C. This is an autoradiogram of a 15% nondenaturing polyacrylamide gel. Lane 1 contains strand 3 of the three-arm junction, and lane 2 contains strands 1 and 2 of the same junction, as markers. Lanes 3−8 have been loaded with equimolar mixtures to form the following structures: lane 3, the three-arm junction, 3_3; lane 4, the three-strand mesojunction, 3_1; lane 5, the conventional four-arm junction, 4_4; lane 6, the four-strand mesojunction, $^14_2$; lane 7, the four-strand mesojunction, $^24_2$; lane 8, the four-strand antijunction, 4_0. Note that the dimer containing the strands of the 3_1 mesojunction is seen in substantial quantities, even at these low strand concentrations. Note also that only a trace of antijunction is seen, and the rest of the material remains in the low-mobility smear. (c, right) The components of the 142-14 mesojunction. This is an autoradiogram of a 12% nondenaturing polyacrylamide gel. Strand concentrations are approximately 20−40 nM. Lanes 1−4 contain the component strands, and lanes 5−8 contain the duplex dimers of the component strands and their Watson−Crick complements, containing radioactive labels in strands 1−4, respectively. Lanes 9−12 contain the mesojunction complex, with radioactive labels in strands 1−4, respectively. It is clear that each of these mesojunction mixtures forms cleanly, without smears or other higher bands.

We found previously that lowering the strand concentrations of these mixtures produced discrete complexes for those molecules containing 16 nucleotide pairs per double-helical component (Du *et al.*, 1992). Figure 2b illustrates the results of examining the mixtures used here on a nondenaturing gel at strand concentrations of 100 nM. The two four-strand mesojunctions, $^14_2$ and $^24_2$, now appear as single discrete bands. However, this is not the case for all species: The lane containing the 3_1 mesojunction continues to show a significant amount of a multimer, which is likely to be a six-strand species. Likewise, only a very small amount of the antijunction (4_0) is seen, and the bulk of the material remains as mixtures of indefinite composition. Increasing the temperature was previously of help, as well, but gels run at 25, 37, and 45 °C revealed the monomeric 3_1 and 4_0 molecules to be absent or only faintly visible, despite the persistence of the multimers (data not shown). Consequently, we have made no attempt to characterize these species by analyses that require a single species in solution. Neither have we attempted to characterize the conventional three-arm branched junction (3_3), because these molecules are already well-known (Guo *et al.*, 1990) and would be interesting here only for comparison with the three-strand mesojunction, 3_1.

The other complex that we wish to characterize is the $^14_2$ mesojunction containing 16 nucleotide pairs in its radial helices and 14 nucleotide pairs in its circumferential helices. Figure 2c illustrates the autoradiogram of a nondenaturing gel containing each of the four strands, the four strands paired with their Watson−Crick complements, and the four-strand complex labeled in each of the four strands. Individual strand concentrations are 100 nM in each lane, and the labeled strand concentrations are 10−20 nM. It is clear that the complex is both stable and discrete under these conditions.

Ferguson Analysis. The slope of the Ferguson (1964) plot of log(mobility) as a function of polyacrylamide concentration yields information about the friction constant of the molecule (Rodbard & Chrambach, 1971). Figure 3a indicates the Ferguson plots for the molecules formed here. The slopes of 4_0, $^14_2$, and $^24_2$ are very similar to each other, despite their different pairing motifs. The slope of the conventional branched junction, 4_4, is slightly larger, but all the slopes are within 10% of each other. The slopes of the previously-studied species containing 16 nucleotide pairs per helix were also roughly parallel, with the exception of the $^14_2$ mesojunction, which was much lower, suggesting greater occlusion of some part of its surface, relative to the other structures. The data here suggest that is not the case when the helices are formed from decamers. All of the plots of these molecules appear to intersect near 8% acrylamide concentration. The plot of the $^14_2$-14 molecule containing 30 nucleotides per strand is shown for comparison. Its higher slope is expected, because its exposed surface area is much larger than the smaller species.

Thermal Transition Profiles. Figure 3b shows the thermal transition profiles of the three complexes formed from strands containing 20 nucleotides and the one complex whose strands contain 30 nucleotides. The data are indicated as T_m (T_{max}), where T_m is the estimated transition midpoint, and T_{max} is the inflection point temperature; the error on these quantities is about 0.5 °C. The complexes whose strands contain 20 nucleotides are very similar in stability, although the conventional branched junction (4_4) [38.1 (38.1) °C] melts slightly higher than the two mesojunctions. This higher stability was seen previously in the analysis of mesojunctions whose strands contain 32 nucleotides (Du *et al.*, 1992). The $^14_2$ [36.6 (38.5) °C] and $^24_2$ [36.5 (38.2, est.) °C] mesojunctions melt at virtually the same temperatures. This is in contrast to the relationship between the two mesojunctions

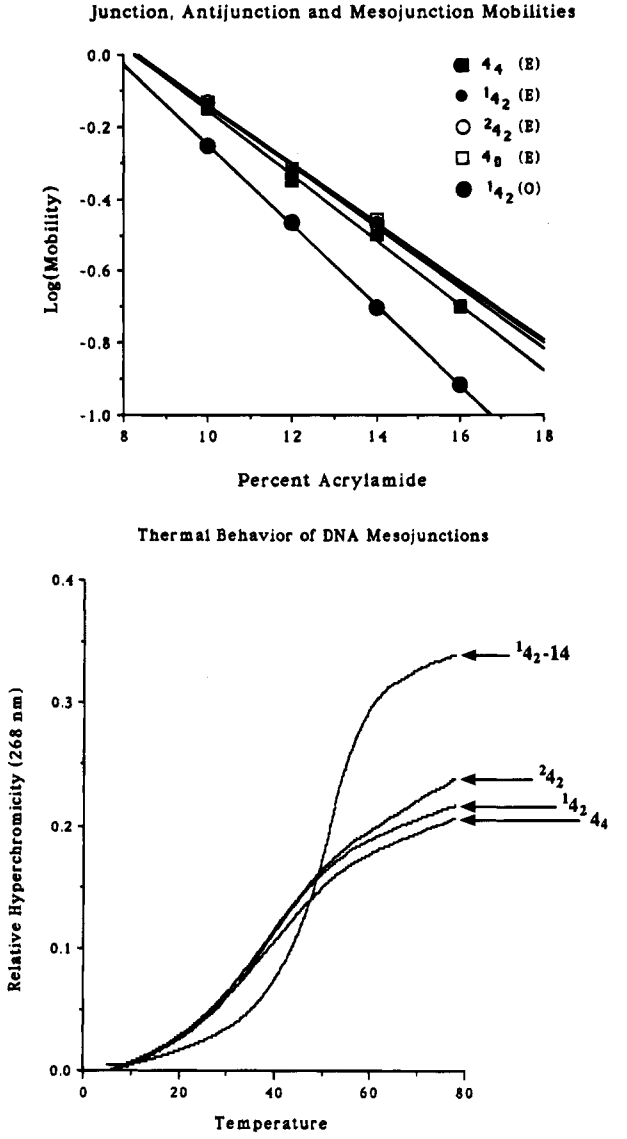

FIGURE 3: Physical characterization of the four-strand complexes. (a, top) Ferguson plots of the four-strand junction, antijunction and mesojunctions. Each of the species in indicated by a coded geometrical object: Open squares for the 4_0 antijunction, filled squares for the 4_4 conventional four-arm branched junction, filled circles for the $^14_2$ mesojunction, open circles for the $^24_2$ mesojunction, and large filled circles for the $^14_2$-14 mesojunction. "E" refers to the complexes containing an even number of half-turns per double helix, and "O" refers to the complex, $^14_2$-14, with an odd number of half-turns per double helix. Not all plot symbols are visible, because of the similarity in the electrophoretic behavior of the complexes. The negative slopes of these plots are 0.0817 and 0.0899 for 4_0 and 4_4, 0.0823 and 0.0847 for $^14_2$ and $^24_2$, and 0.1114 for $^14_2$-14. (b, bottom) Thermal transition profiles. Each curve has been smoothed by a 23-point interpolation. Relative hyperchromicity is calculated as $[OD_{268}(T)/OD_{268}(T_o) - 1]$, where $T_o = 4$ °C. The curves have been obtained at 0.1 °C intervals. The conventional junction whose strands contain 20 nucleotides has a slightly higher transition midpoint than the mesojunctions of comparable length. The mesojunction whose strands contain 30 nucleotides is the most stable and denatures most cooperatively.

previously studied: Stacking some of the domains of the three-half-turn $^24_2$ mesojunction implies destabilization of base pairs in other domains in order to relieve strain, but this is not required in the molecule studied here. The similarity of all the melting temperatures indicates that the three complexes base pair to a similar extent. Derivative plots indicate small premelting transitions in the vicinity of 20 °C in all three molecules, although the transition is least prominent in $^24_2$ (data not shown). The thermal transition profile of the $^14_2$-14 mesojunction is shown for comparison. The larger size of its domains results, as expected, in a higher melting temperature [49.7 (51.3) °C] that is also more cooperative.

Hydroxyl Radical Analysis. Hydroxyl radical autofootprinting has been extremely useful in providing structural information about branched junctions (Churchill *et al.*, 1988; Chen *et al.*, 1988; Wang *et al.*, 1991; Kimball *et al.*, 1990) and double crossover molecules (Fu & Seeman, 1993; Zhang *et al.*, 1993; Zhang & Seeman, 1994) as well as in the analysis of the previously characterized antijunction and mesojunctions (Du *et al.*, 1992). These experiments are performed by labeling a component strand of the complex and exposing it to hydroxyl radicals. The key feature noted in these experiments is decreased susceptibility to attack in the comparison between the pattern seen when the strand is part of the complex, relative to the pattern derived from duplex DNA. Decreased susceptibility is interpreted to suggest that access to the hydroxyl radical may be limited by steric factors at the sites where it is noted. Likewise, similarity to the duplex pattern at points of potential flexure is assumed to indicate that the strand has adopted a helical structure in the complex, even though this is not required by the secondary structure. For example, Churchill *et al.* (1988) concluded that the four arms of a Holliday junction analog assort themselves into two stacking domains because the attack patterns of two strands are identical between the junction and duplex DNA. In previous work with antijunctions and mesojunctions (Du *et al.*, 1992) and junctions with large numbers of arms (Wang *et al.*, 1991), protection at points between helices has been taken to indicate that the strand switches between helical domains.

Figure 4 illustrates scans of the strands of the three mesojunctions ($^14_2$, $^14_2$, and $^14_2$-14) in comparison with duplex DNA. The conventional branched junction (4_4), whose pattern is well known (Churchill *et al.*, 1988), is shown as a control. Representative scans are shown, and a semiquantitative interpretation of the protection seen on the complex, relative to the duplex. We use a scale of three different sizes of triangles at individual sites to indicate the extent of protection. Large triangles indicate protection of 25% or greater. Intermediate triangles represent protection between 10% and 25%. Small triangles represent protection below 10%. All protection seen is reproducible. The triangles represent the average protection seen, which may differ slightly from that seen in the scan shown.

The Four-Arm Branched Junction. Figure 4a illustrates the pattern of the four-arm branched junction, 4_4. This junction has been derived from the well-known junction, J1 (Seeman & Kallenbach, 1983), whose hydroxyl radical pattern has been established (Churchill *et al.*, 1988). The crossover points on strands 2 and 4 are strongly protected at the central positions (10 and 11) and somewhat more weakly at the residue 5′ to that site (position 9). Weaker protection is also seen four nucleotides 3′ to the crossover point on the noncrossover strands. The protection sites seen here are similar to those noted previously and are consistent with parallel or antiparallel two-domain models of the junction (Churchill *et al.*, 1988; Kimball *et al.*, 1990).

The Four-Strand Mesojunction $^14_2$. Figure 4b shows the hydroxyl radical cleavage pattern for this mesojunction. Strong protection is seen on strands 2 and 4 in the vicinity of the central positions, but none is seen at these sites on

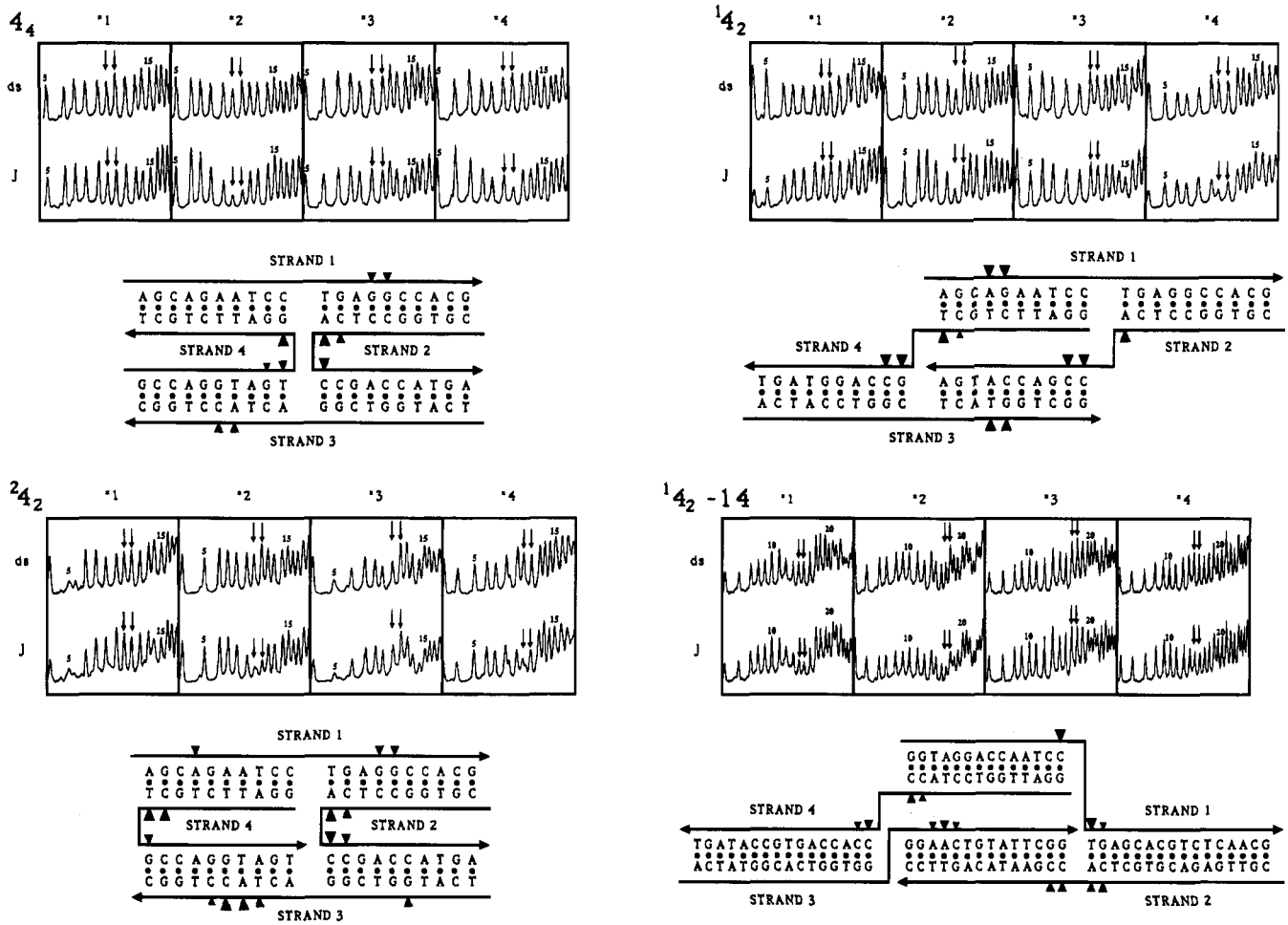

FIGURE 4: Hydroxyl radical cleavage patterns for a four-strand junction and three four-strand mesojunctions. Each panel of this figure contains two parts, a direct comparison of the hydroxyl radical sensitivity of an individual strand in its complex (J), compared with the same strand paired to its Watson–Crick complement (ds). The two nucleotides of each strand that connect between helices are indicated by two arrows. Protection at individual sites is indicated in the schematic diagram below the comparison by triangular indicators, with the extent of protection indicated qualitatively by the size of the triangle: The largest triangles correspond to protection greater than 25%, relative to duplex, intermediate triangles are protection between 10% and 25%, and small triangles are protection less that 10% relative to duplex. Except for $^{2}4_{2}$, protection was triply reproduced before being scored. (a, top left) The 4_4 junction. The features seen here are similar to those noted previously for this type of complex (Churchill *et al.*, 1988). (b, top right) The $^{1}4_{2}$ mesojunction. (c, bottom left) The $^{2}4_{2}$ mesojunction. (d, bottom right) The $^{1}4_{1}$-14 mesojunction.

strands 1 and 3. However, strands 1 and 3 do exhibit protection four nucleotides 3′ to the crossover of strand 4. The lack of protection at the central positions of strands 1 and 3 suggests that both the 5′ and 3′ portions of the strands are part of the same helical domain. If this is the case, the two strands are parallel, similar to the helical strands of a DPE double crossover molecule (Fu & Seeman, 1993); this is a molecule containing two crossovers, in which the crossovers are separated by an even number of double-helical half-turns. The protection at the sites four nucleotides 3′ to the strand 4 crossover seen in this mesojunction is analogous to the protection seen in the DPE molecule. It arises from the mutual occlusion of the two strands one minor groove spacing 3′ to the crossover site.

The similarity to the DPE double crossover structure (Fu & Seeman, 1993) can be seen in Figure 5a. The two strands drawn with thicker lines are parallel in both structures, and the other strands are antiparallel to them. The major grooves and minor grooves align exactly in each molecule. The molecules differ in that there is only a single strand crossing over at each connection between double-helical domains in the mesojunction, but two strands effect the crossover in both sites in the DPE molecule.

The Four-Strand Mesojunction $^{2}4_{2}$. We have previously pointed out (Du *et al.*, 1992) that the $^{2}4_{2}$ mesojunction bears a strong similarity to a Holliday junction tethered (Kimball *et al.*, 1990) to assume an antiparallel conformation. The molecule studied previously, with three half-turns per helix, suffered from incompatibility of twists in the two domains, so that no discrete structure could be determined for it. Switching to a molecule with only two half-turns per helix has solved that problem. The protection pattern is very similar to that seen for antiparallel junctions (Kimball *et al.*, 1990) or for antiparallel double crossover molecules (Fu & Seeman, 1993). Two strands (1 and 3) are helical, as shown by the lack of protection in the vicinities of their potential crossover points. The other two strands (2 and 4) are protected strongly at their crossover sites. The helical strands show protection of varying intensity four or five nucleotides 3′ to crossover sites.

The structure of the molecule is shown in Figure 5b, where it is compared with the structure of a DAE double crossover molecule. The key similarity is the antiparallel orientations of the helical strands (1 and 3) in each molecule. The DAE molecule contains an extra strand (5), shown on the left of Figure 5b. In addition, strand 4 is phased differently. As

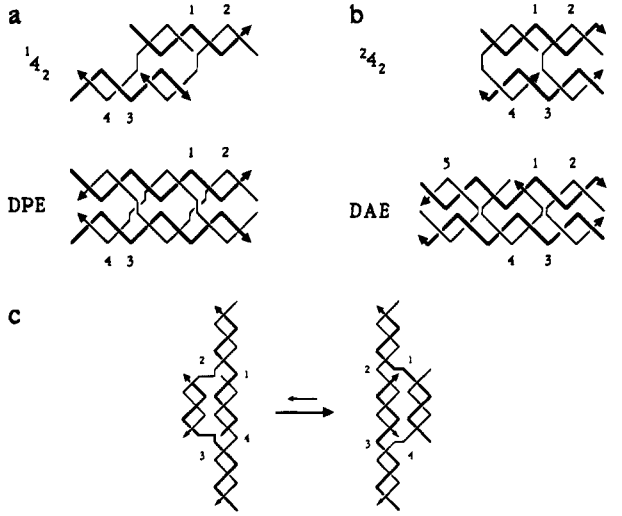

FIGURE 5: Structural models for the mesojunctions studied. In each panel, the structures are drawn schematically with strands of two different thicknesses, to emphasize clarity and symmetry. Arrowheads indicate the 3′ ends of strands. Major and minor grooves are indicated. (a) The $^{1}4_{2}$ mesojunction. This panel compares the structure derived from Fe(II)EDTA^{2-} footprinting with the structure of the previously studied double crossover molecule, DPE (Fu & Seeman, 1993). The strands are numbered in the same positions, for clarity. Note that the parallel orientations of the thick helical strands lead ideally to exact juxtaposition of strands, so that major and minor groves face each other across the central domain boundary. (b) The $^{2}4_{2}$ mesojunction. This panel compares the structure derived from Fe(II)EDTA^{2-} footprinting with the structure of the previously studied double crossover molecule, DAE (Fu & Seeman, 1993). The strands are numbered in the same positions, for clarity, although there is a fifth strand associated with the DAE molecule. Note that the antiparallel orientations of the thick helical strands lead to major and minor grooves facing each other across the domain boundary. (c) The $^{1}4_{2}$-14 mesojunction. The equilibrium characterizing this structure is shown, with the dominant isomer indicated by the thicker arrow in the center of the panel. The structure on the right is the mesojunction equivalent of a DPON (two minor grooves, one major groove in the central helices) double crossover molecule, and the structure on the left is the mesojunction equivalent of a DPOW (two major grooves, one minor groove in the central helices) double crossover molecule (Fu & Seeman, 1993). The right-angled kinks in the molecule on the left are intended to indicate the difficulty of forming a DPOW-type molecule with 14 nucleotides in the central helices.

with $^{1}4_{2}$, these differences result in single, rather than reciprocal crossovers between the two helical domains. It is worth pointing out that the antiparallel orientations of the helical domains result in major grooves of one domain facing minor grooves of the other. As in the case of Holliday junctions (Seeman & Kallenbach, 1994) and double crossover molecules (Fu & Seeman, 1993), this situation staggers the strands on the domain interface and is expected to be more stable than the direct juxtaposition of strands seen in the parallel molecules shown in Figure 5a.

The Four-Strand Mesojunction $^{1}4_{2}$-14. In our previous work with mesojunctions, we found that the $^{1}4_{2}$ mesojunction containing three half-turns of DNA per helical domain formed a stacking structure like that shown on the left of Figure 5c (Du *et al.*, 1992). There are two double crossover molecules analogous to this class of mesojunctions, DPOW and DPON. Both contain an odd number of half-turns between crossover points, but the extra half-turn is a major (wide) groove separation in the case of DPOW, and it is a minor (narrow) groove separation in the case of DPON (Fu & Seeman, 1993). The molecule previously studied is analogous to a DPOW double crossover molecule, because it contained 16 nucleotide pairs per helical domain. It was clear that forming the structure on the right of Figure 5c would result in torsional stress in that molecule. Here, we have constructed the four-strand mesojunction $^{1}4_{2}$-14, containing 14 nucleotide pairs in its circumferential domains, in order to see if we could induce the molecule to prefer the DPON-like conformer. The reason to expect this to shift the equilibrium is that 14 nucleotides generate an extra minor groove separation, corresponding to the structure on the right.

We have been partially successful. In the DPON-like conformer, one expects protection at the crossover points of strands 1 and 4 and none at the comparable points of strands 2 and 3. We see the protection we expect, but we also see protection on strand 2. This is reminiscent of the protection seen on the previous molecule, where some protection was seen on all strands at their crossover points, suggesting an equilibrium between the two conformers. In addition to crossover protection, protection is seen on strand 3, one minor-groove separation 3′ to the crossover involving strand 4, suggesting the occlusion of that site by the comparable position on strand 1.

DISCUSSION

Complex Formation. In contrast to the antijunction and mesojunctions constructed with three half-turns per helix, we have not been able to construct all of the species indicated in Figure 1b, when the size of the helices has been reduced to a single turn. In particular, the 3_1 mesojunction and the 4_0 antijunction have proved intractable to our efforts. Model building (Seeman, 1988) suggests that the monomer of the 3_1 mesojunction is incompatible with the stacking interactions that seem to dominate all the unusual structures studied to date: Branched junctions (Churchill *et al.*, 1988; Wang *et al.*, 1991) and double crossovers (Fu & Seeman, 1993) as well as antijunctions and mesojunctions (Du *et al.*, 1992). By contrast, model building suggests that the 4_0 antijunction can be stabilized by stacking interactions between its domains. The structure one derives is similar to that shown in Figure 5b for $^{2}4_{2}$, except that strand 2 is rephased, so that its gap is at the center of the molecule, rather than on the end at the right side. This rephasing creates a 2-fold symmetric object, which also could stack the other way, with strands 1 and 3 forming the crossovers. The study involving helices containing 16 nucleotide pairs also found antijunctions extremely difficult to isolate as a single species.

Hydroxyl Radical Characterization of Mesojunctions. The structures derived for the two mesojunctions constructed from strands containing 20 nucleotides are in agreement with those predicted from model building that takes topology into account (Seeman, 1988). The $^{1}4_{2}$ mesojunction forms a structure containing two stacking domains, each the result of stacking two helices. This structure is in contrast to that formed from the previously studied mesojunction (Du *et al.*, 1992), in which the helical domains contain three helices and one helix, rather than two and two. This is not surprising, since the earlier structure is closely related to a DPOW double crossover structure, and the one studied here is related to a DPE molecule.

The other $^{1}4_{2}$ molecule studied here, $^{1}4_{2}$-14 is related to a DPON molecule, and appears to form a structure whose two stacking domains contain three helices and one helix, respectively. However, the helices involved are the opposite of those in the DPOW molecule. The single helical domain

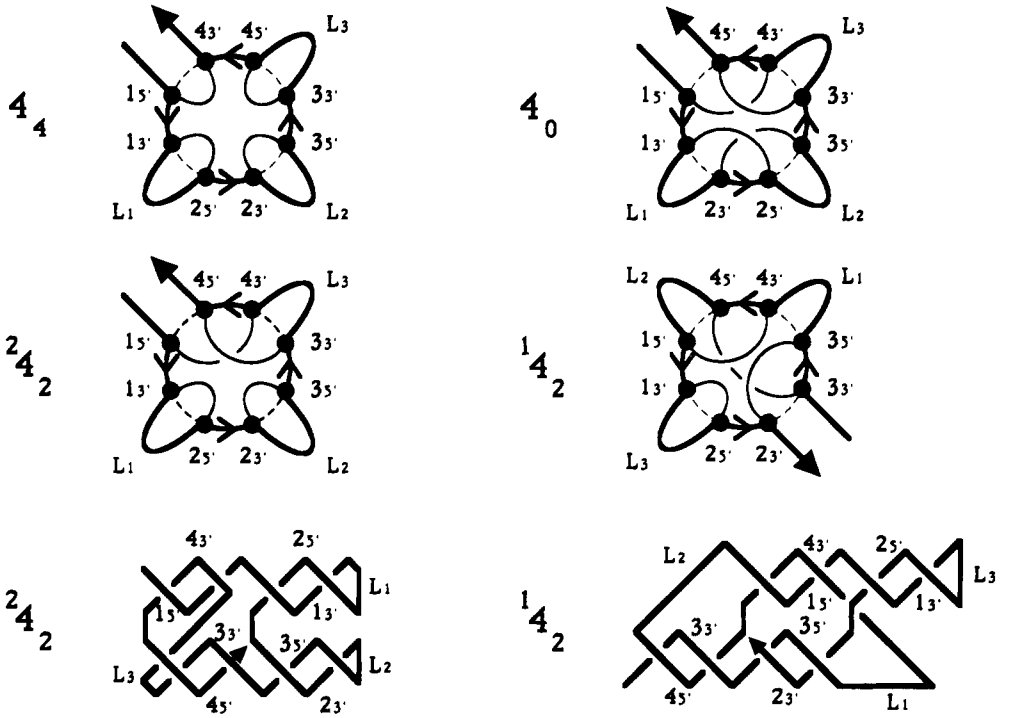

FIGURE 6: Molecular graphs and models that contain unusual structures embedded in long single strands. The four diagrams in the top and central portions of this figure represent a four-strand junction, 4_4, an antijunction, 4_0, and the two mesojunctions, $^{1}4_2$ and $^{2}4_2$, which have all been embedded into long single strands. The 3′ end of each single strand is represented by a line ending in an arrowhead pointing away from the center of the figure, and the 5′ end is represented by a line parallel to it. The polynucleotide backbone is represented by thick lines external to or on the circumference of a circle formed by a dotted line. The arrowheads along this line represent the 5′→3′ direction of the strand. The parts on the circumference of the circle correspond to the four individual strands that make up a junction, mesojunction, or antijunction. Loops have been added to the structures to form a single strand; these are labeled by their order from the 5′ end, L_1, L_2, and L_3. Their 5′ and 3′ attachment points are arbitrary and have been made sequential only for the sake of simplicity. Each hydrogen bonding region is represented by a single dot, corresponding to a vertex on the molecular graph. The dots are labeled by the names of the strand halves that would form a four-arm branched junction, as described in Materials and Methods, Sequence Design: $1_{5'}$, $1_{3'}$, $2_{5'}$, $2_{3'}$, $3_{5'}$, $3_{3'}$, $4_{5'}$, $4_{3'}$. Pairing between dots is illustrated by a thin arc connecting two dots on the interior of a dotted circle. The interior of the circle represents secondary structure, whereas its circumference and exterior represent primary structure. For simplicity, no loops have been added between two successive dots on the circumference of the circle. In the case of the branched junction, 4_4, the arcs do not overlap. The arcs do intersect in the cases of the mesojunctions and the antijunction, because the pairing portions have been reversed to yield the mesojunctions or antijunction. The node senses at arc intersection points are arbitrary. The bottom portion of the figure illustrates the two structural models from Figure 5a,b as they have been incorporated into the single strands whose molecular graphs are above them; the arrowheads represent the 3′ ends. The structures and topologies of the linkers (L_1, L_2, and L_3) are arbitrary, but the structures of the helical domains conform with the structural models derived. The strand segments are labeled identically to the molecular graphs above them.

contains the 5′ ends of its two strands, whereas the single helical domain of the DPOW-related $^{1}4_2$ mesojunction contains the 3′ ends of its two strands. The protection noted on strand 2 of $^{1}4_2$-14 indicates that this structure is not formed cleanly; it is likely that some component of the structure corresponding to the DPOW-like mesojunction is present, just as some of the DPON-like mesojunction was present in the mesojunction with 16 nucleotides per circumferential helix.

The $^{2}4_2$ mesojunction characterized here is the first one for which a discrete structure has been proposed. The $^{2}4_2$ mesojunction with three half-turns per helix contained twists so incompatible with a stable structure that the hydroxyl radical attack pattern was uninterpretable (Du *et al.*, 1992). The structure derived here, however, is stable, readily characterized, and compatible with model building. As noted above, it is very closely related to the structure of a DAE-like double crossover structure. It differs from the two-domain $^{1}4_2$ mesojunction discussed above in that its helical strands are antiparallel rather than parallel. Antiparallel branched junctions and double crossover molecules appear to be more stable than parallel ones (Lu *et al.*, 1991; Fu & Seeman, 1993). Nevertheless, as noted above, at the high concentrations used in Figure 2a, the dimer of $^{2}4_2$ is prominent and the trimer is seen, but only a small amount of the $^{1}4_2$ dimer is seen. Possibly this is due to fewer interdomain interactions.

Biological Structures. Relationship of Mesojunctions to Recombination Intermediates. The mesojunctions studied here form crossover structures, which are related to the crossover structures encountered in genetic recombination. However, they are not reciprocal crossover structures, because only a single strand of DNA connects each helical domain to its neighbor at any given crossover point. This situation contrasts with double crossover structures (Thaler & Stahl, 1988; Sun *et al.*, 1991; Fu & Seeman, 1993), in which each connection is formed by two intact strands. The second strand is replaced here with the 5′ and 3′ ends of two separate strands. Thus, these molecules may represent models for strand-invasion structures. It is a poor analogy to say that they resemble double crossover molecules in which one of the crossovers has been nicked: One must neglect twist and, for parallel molecules, helical strand polarity, in order for this analogy to hold.

Mesojunctions or Antijunctions as Elements of Secondary Structure. It is useful to recall that antijunctions and mesojunctions were first discovered as components of single-stranded nucleic acid knots (Seeman, 1992; Du *et al.*, 1992;

Seeman *et al.*, 1993). Hence, they may occur within the secondary structures of long single-stranded nucleic acids, particularly RNA. Liang and Mislow (1994) have recently modeled interstrand disulfide bonds in proteins as connected vertices on a molecular graph whose main axis is the polypeptide backbone. In the upper and middle portions of Figure 6 we use a modification of this notation, combined with the circular notation of ten Dam *et al.* (1992), to represent the secondary structures of a nucleic acid branched junction, an antijunction, and two mesojunctions containing four strands: We condense each of the two complementary strands of a double helix to a single vertex, represented as a dot on this molecular graph. Each dot is labeled with the same notation used above (see Materials and Methods: Sequence Design) to designate the sequence of half of a pairing strand ($1_{5'}$, $1_{3'}$, $2_{5'}$, $2_{3'}$, $3_{5'}$, $3_{3'}$, $4_{5'}$, $4_{3'}$). Double helix formation by hydrogen bonding is represented by a thin arc within a dotted circle, and the polynucleotide backbone is represented by a thick line on the circumference or outside the circle. Thus, the interior of the dotted circle corresponds to secondary structural interactions, but its circumference and exterior represent primary structure. The condensation of helical single strands to dots elides topological linking, but it provides a convenient shorthand to denote secondary interactions. The secondary structures of single-stranded nucleic acid molecules are usually modeled as a series of hairpins (Jaeger *et al.*, 1989; Zuker, 1989; Draper, 1992). A molecule that embeds the four helical arms of a conventional branched junction, such as a tRNA cloverleaf (e.g., Kim *et al.*, 1974) (neglecting the nucleotides between stems) or a DNA shamrock (Mueller *et al.*, 1988) fits this paradigm. Such a structure is represented in the upper left of the diagram, and is labeled 4_4. The key feature of this simple structure is that *the arcs representing hydrogen bonding do not intersect.*

The inversion of pairing sequences discussed above in the section on the sequence design of antijunctions and mesojunctions from conventional branched junctions *necessarily generates intersections among arcs* that connect these points on the molecular graph. The $^2{4_2}$ mesojunction contains two arcs that cross, the $^1{4_2}$ mesojunction contains three arcs that cross, and the 4_0 antijunction contains four arcs that cross. Ten Dam *et al.* (1992) have pointed out that intersections within the circle correspond to complex arrangements within the strand, such as those generated by pseudoknots. For example, the pairing of helices P3 and P7 of the *Tetrahymena* ribozyme (Burke *et al.*, 1987) generates an arc intersection on a molecular graph that contains 13 other noncrossing (but sometimes nested) arcs.

The importance of the coaxial stacking of helices in RNA structures has recently received much attention as a source of stability (Murphy *et al.*, 1994; Walter & Turner, 1994; Walter *et al.*, 1994). As noted above, this stacking is well known in DNA molecules (Churchill *et al.*, 1988; Lilley & Clegg, 1993; Seeman & Kallenbach, 1994), and it has been found here between the helical sections of DNA mesojunctions. At the bottom of Figure 6, we have connected by loops the strands of the $^2{4_2}$ and $^1{4_2}$ mesojunctions, to correspond to both the models of Figure 5 (a and b) and to the connectivities shown in the central panels of Figure 6. The connectivities, topologies, and structures of the loops are arbitrary, but the stacking diagrams indicate the types of structures these DNA molecules could form in a connected single-stranded context. Similar characterization of RNA molecules containing these topological features would reveal structural information of importance to understanding their role within the cell.

ACKNOWLEDGMENT

We thank Dr. Richard D. Sheardy for valuable discussions and assistance with the measurement of thermal denaturation profiles on his spectrophotometer (supported by PRF Grant 27471-AC7 and NIH Grant GM-51069 to him) and Dr. Luis A. Marky for valuable discussions of the thermal data. We also thank Dr. Shou Ming Du for valuable discussions about the sequences of these molecules and Dr. Siwei Zhang for discussions about Fe(II)EDTA^{2-} autofootprinting. The support of Biomolecular Imaging on the NYU campus by the W. M. Keck Foundation is gratefully acknowledged.

REFERENCES

Burke, J. M., Belfort, M., Cech, T. R., Davies, R. W., Schweyen, R. J., Shub, D. A., Szostak, J. W., & Tabak, H. F. (1987) *Nucleic Acids Res. 15*, 7217−7221.

Caruthers, M. H. (1985) *Science 230*, 281−285.

Chen, J.-H., Churchill, M. E. A., Tullius, T. D., Kallenbach, N. R., & Seeman, N. C. (1988) *Biochemistry 27*, 6032−6038.

Churchill, M. E. A., Tullius, T. D., Kallenbach, N. R., & Seeman, N. C. (1988) *Proc. Natl. Acad. Sci. U.S.A. 85*, 4653−4656.

Draper, D. E. (1992) *Acc. Chem. Res. 25*, 201−207.

Du, S. M., Zhang, S., & Seeman, N. C. (1992) *Biochemistry 31*, 10955−10963.

Ferguson, K. A. (1964) *Metabolism 13*, 985−1002.

Fu, T.-J., & Seeman, N. C. (1993) *Biochemistry 32*, 3211−3220.

Guo, Q., Lu, M., Churchill, M. E. A., Tullius, T. D., & Kallenbach, N. R. (1990) *Biochemistry 29*, 10927−10934.

Hoess, R., Wierzbicki, A., & Abremski, K. (1987) *Proc. Natl. Acad. Sci. U.S.A. 84*, 6840−6844.

Holliday, R. (1964) *Genet. Res. 5*, 282−304.

Jaeger, J. A., Turner, D. H., & Zuker, M. (1989) *Proc. Natl. Acad. Sci. U.S.A. 86*, 7706−7710.

Kallenbach, N. R., Ma, R.-I., & Seeman, N. C. (1983) *Nature (London) 305*, 829−831.

Kang, C. H., Zhang, X., Ratliff, R., Moyzis, R., & Rich, A. (1992) *Nature (London) 356*, 126−131.

Kim, S.-H., Suddath, F. L., Quigley, G. J., McPherson, A., Sussman, J. L., Wang, A. H.-J., Seeman, N. C., & Rich, A. (1974) *Science 185*, 435−440.

Kimball, A., Guo, Q., Lu, M., Cunningham, R. P., Kallenbach, N. R., Seeman, N. C., & Tullius, T. D. (1990) *J. Biol. Chem. 265*, 6544−6547.

Kitts, P. A., & Nash, H. A. (1987) *Nature (London) 329*, 346−348.

Liang, C., & Mislow, K. (1994) *J. Am. Chem. Soc. 116*, 3588−3592.

Lilley, D. M. J., & Clegg, R. M. (1993) *Annu. Rev. Biophys. Biomol. Struct. 22*, 299−328.

Lu, M., Guo, Q., Seeman, N. C., & Kallenbach, N. R. (1991) *J. Mol. Biol. 221*, 1419−1432.

Ma, R.-I., Kallenbach, N. R., Sheardy, R. D., Petrillo, M. L., & Seeman, N. C. (1986) *Nucleic Acids Res, 14*, 9745−9753.

Maxam, A. M., & Gilbert, W. (1977) *Proc. Natl. Acad. Sci. U.S.A. 74*, 560−564.

Mueller, J. E., Kemper, B., Cunningham, R. P., Kallenbach, N. R., & Seeman, N. C. (1988) *Proc. Natl. Acad. Sci. U.S.A. 85*, 9441−9445.

Murphy, F. L., Wang, Y.-H., Griffith, J. D., & Cech, T. R. (1994) *Science 265*, 1709−1702.

Nunes-Duby, S. E., Matsumoto, L., & Landy, A. (1987) *Cell 50*, 779−788.
Rodbard, D., & Chrambach, A. (1971) *Anal. Biochem. 40*, 95−134.
Seeman, N. C. (1982) *J. Theor. Biol. 99*, 237−247.
Seeman, N. C. (1988) *J. Biomol. Struct. Dyn. 5*, 997−1004.
Seeman, N. C. (1992) *Mol. Eng. 2*, 297−307.
Seeman, N. C., & Kallenbach, N. R. (1983) *Biophys. J. 44*, 201−209.
Seeman, N. C., & Kallenbach, N. R. (1994) *Annu. Rev. Biophys. Biomol. Struct. 23*, 53−86.
Seeman, N. C., Chen, J., Du, S. M., Mueller, J. E., Zhang, Y., Fu, T.-J., Wang, H., Wang, Y., & Zhang, S. (1993) *New J. Chem. 17*, 739−755.
Smith, F. W., & Feigon, J. (1992) *Nature (London) 356*, 164−168.
Sun, H., Treco, D., & Szostak, J. W. (1991) *Cell 64*, 1155−1161.
Tang, C. K., & Draper, D. E. (1989) *Cell 57*, 531−536.
ten Dam, E., Pleij, K., & Draper, D. E. (1992) *Biochemistry 31*, 11665−11676.
Thaler, D. S., & Stahl, F. W. (1988) *Annu. Rev. Genet. 22*, 169−197.
Tullius, T. D., & Dombroski, B. (1985) *Science 230*, 679−681.
Tullius, T. D., & Dombroski, B. (1986) *Proc. Natl. Acad. Sci. U.S.A. 83*, 5469−5473.
Walter, A. E., & Turner, D. H. (1994) *Biochemistry 33*, 12715−12719.
Walter, A. E., Turner, D. H., Kim, J., Lyttle, M. H., Müller, P., Mathews, D. H., & Zuker, M. (1994) *Proc. Natl. Acad. Sci. U.S.A. 91*, 9218−9222.
Wang, Y., Mueller, J. E., Kemper, B., & Seeman, N. C. (1991) *Biochemistry 30*, 5667−5674.
Watson, J. D., & Crick, F. H. C. (1953) *Nature (London) 171*, 737−738.
Zhang, S., & Seeman, N. C. (1994) *J. Mol. Biol. 238*, 658−668.
Zhang, S., Fu, T.-J., & Seeman, N. C. (1993) *Biochemistry 32*, 8062−8067.
Zuker, M. (1989) *Science 244*, 48−52.

BI9421634